

A NUMERICAL METHOD FOR SOLVING THE OLDROYD-B MODEL FOR 3D FREE SURFACE FLOWS

Murilo F. Tomé *, **Antonio Castelo***, **Fernando M. Federson *** and **José A. Cuminato ***

*Grupo de Mecânica dos Fluidos Computacional

Departamento de Ciências de Computação e Estatística - ICMC - USP

Av. do Trabalhador São-Carlense, 400 São Carlos - SP, Brazil - CEP 13560-970

e-mail: (murilo, fernando, castelo, jacumina)@icmc.usp.br, web page: <http://www.lcad.icmc.usp.br>

Key Words: Oldroyd-B, Viscoelastic Flow, Finite Difference, Marker-and-Cell, Free Surface.

Abstract. *This work presents a numerical method for solving three-dimensional viscoelastic free surface flows governed by the Oldroyd-B constitutive equation. It is an extension to three dimensions of the technique introduced by Tomé et al.¹ The governing equations are solved by a finite difference method on a 3D-staggered grid. Marker particles are employed to describe the fluid providing the visualization and the location of the fluid free surface. As currently implemented, the numerical method presented in this work can simulate three-dimensional free surface flows of an Oldroyd-B fluid. The numerical technique presented in this paper is validated by using an exact solution of the flow of an Oldroyd-B fluid inside a pipe. Numerical simulation of the extrudated swell is given.*

1 INTRODUCTION

The numerical treatment of free surface flows is an area that has attracted the attention of many researchers over the last two decades and still presents several challenges: the flow is transient, non-isothermal, non-Newtonian and possess multiple free surfaces. Nonetheless, a number of researchers have developed numerical methods capable of simulating free surface flows that can be applied to the design and manufacture of many industrial processes. Among the numerical techniques employed the finite difference method has been employed by various researchers.²⁻⁵ The development of numerical methods for simulating viscoelastic flows has been in area of intense research. However, the majority of papers published can only cope with confined flows such as the numerical simulation of the flow in a abrupt contraction (see Yoo and Na,³ Mompean and Deville,⁶ Xue et al.,⁷ Pinho,⁸ Phillips and Williams⁹) which has been investigated in 2 and 3 dimensions. Numerical methods for viscoelastic flows with a free surface have also been investigated.¹⁰⁻¹³ However, due to the complexity of these flows, only problems having a small free surface deformation or steady state problems are usually treated. Recently, Tomé et al.¹ developed a numerical method for solving time-dependent viscoelastic free surface flows. More precisely, Tomé et al.¹ presented a numerical technique for simulating two-dimensional free surface flows of a fluid described by the Oldroyd-B constitutive equation. Numerical results for the extrudate swell and the jet buckling for high Weissenberg numbers were obtained. In this work we use the ideas presented by Tomé et al.¹ and develop a numerical method for solving the governing equations for the three-dimensional flow of an Oldroyd-B fluid. The technique employs the finite difference method on a staggered grid and the fluid free surface is modelled by the Marker-and-Cell method. The numerical method presented in this paper is validated by simulating the flow of an Oldroyd-B fluid in pipe and compared with its analytic solution.

2 GOVERNING EQUATIONS

The governing equations of incompressible flows are the mass conservation equation and the equation of motion which can be written as

$$\frac{\partial v_i}{\partial x_i} = 0, \quad (1)$$

$$\rho \frac{Dv_i}{Dt} = -\frac{\partial p}{\partial x_i} + \frac{\partial \sigma_{ik}}{\partial x_k} + \rho g_i, \quad (2)$$

where t is the time, $v_i = (u, v, w)^T$ is the velocity vector, $x_i = (x, y, z)^T$ is the position vector, p is the pressure, σ_{ik} is the extra-stress tensor, ρ is the fluid density and $g_i = (g_x, g_y, g_z)^T$ is the gravity field. In this work the fluid is described by the Oldroyd-B model so that we employ the following constitutive equation for σ_{ik}

$$\sigma_{ik} + \lambda_1 \overset{\nabla}{\sigma}_{ik} = 2\mu_0 \left(d_{ik} + \overset{\nabla}{d}_{ik} \right), \quad (3)$$

where $d_{\mathbf{ik}}$ is the rate-of-deformation tensor

$$d_{\mathbf{ik}} = \frac{1}{2} \left(\frac{\partial v_i}{\partial x_k} + \frac{\partial v_k}{\partial x_i} \right), \quad (4)$$

μ_0 is the fluid viscosity, λ_1, λ_2 are time constants defining the Oldroyd-B model and $(\overset{\nabla}{\bullet})$ represents the upper convected derivative defined by

$$\overset{\nabla}{\sigma}_{\mathbf{ik}} = \frac{\partial \sigma_{\mathbf{ik}}}{\partial t} + \frac{\partial v_m \sigma_{\mathbf{ik}}}{\partial x_m} - \frac{\partial v_i}{\partial x_m} \sigma_{mk} - \frac{\partial v_k}{\partial x_m} \sigma_{im}. \quad (5)$$

To solve equations (1)-(3) we employ the change of variables (known as EVSS method¹⁴)

$$\sigma_{\mathbf{ik}} = 2\mu_0 \left(\frac{\lambda_2}{\lambda_1} \right) d_{\mathbf{ik}} + S_{\mathbf{ik}} \quad (6)$$

where $S_{\mathbf{ik}}$ represents the non-Newtonian contribution to the extra-stress tensor. Introducing (6) into equations (2) and (3) we obtain the following equations (we employed the non-dimensional form where $v_i = U\bar{v}_i$, $p = (\rho U^2)\bar{p}$, $S_{\mathbf{ik}} = (\rho U^2)\bar{S}_{\mathbf{ik}}$, $t = (L/U)\bar{t}$, $x_i = L\bar{x}_i$, the bars have been dropped for clarity)

$$\rho \frac{Dv_i}{Dt} = -\frac{\partial p}{\partial x_i} + \frac{1}{Re} \left(\frac{\lambda_2}{\lambda_1} \right) \frac{\partial}{\partial x_k} \left(\frac{\partial v_i}{\partial x_k} \right) + \frac{\partial S_{\mathbf{ik}}}{\partial x_k} + \rho g_i \quad (7)$$

and

$$S_{\mathbf{ik}} + We \overset{\nabla}{S}_{\mathbf{ik}} = \frac{2}{Re} \left(1 - \frac{\lambda_2}{\lambda_1} \right) d_{\mathbf{ik}}. \quad (8)$$

where $Re = \frac{\rho UL}{\mu}$, $Fr = \frac{U}{\sqrt{Lg}}$ and $We = \lambda_1 \frac{U}{L}$ are the Reynolds, Froude and Weissenberg numbers, respectively. We consider three-dimensional flows. Thus, the mass equation (1) together with the momentum equation (7) and the Oldroyd-B constitutive equation (8), consist of a system of partial differential equations with 10 equations for the unknowns $u, v, w, p, S^{xx}, S^{xy}, S^{xz}, S^{yy}, S^{yz}, S^{zz}$. By using Cartesian coordinates, the mass conservation equation (1) becomes

$$\frac{\partial u}{\partial x} + \frac{\partial v}{\partial y} + \frac{\partial w}{\partial z} = 0, \quad (9)$$

while the x -component of equations (7) and (8) can be written as

$$\begin{aligned} \frac{\partial u}{\partial t} + \frac{\partial(u^2)}{\partial x} + \frac{\partial(vu)}{\partial y} + \frac{\partial(wu)}{\partial z} = & -\frac{\partial p}{\partial x} + \frac{1}{Re} \left(\frac{\lambda_2}{\lambda_1} \right) \left[\frac{\partial^2 u}{\partial x^2} + \frac{\partial^2 u}{\partial y^2} + \frac{\partial^2 u}{\partial z^2} \right] \\ & + \frac{\partial S^{xx}}{\partial x} + \frac{\partial S^{xy}}{\partial y} + \frac{\partial S^{xz}}{\partial z} + \frac{1}{Fr^2} g_x, \end{aligned} \quad (10)$$

$$\begin{aligned} S^{xx} + We \left[\frac{\partial S^{xx}}{\partial t} + \frac{\partial(uS^{xx})}{\partial x} + \frac{\partial(vS^{xx})}{\partial y} + \frac{\partial(wS^{xx})}{\partial z} - 2 \left(\frac{\partial u}{\partial x} S^{xx} + \frac{\partial u}{\partial y} S^{xy} + \frac{\partial u}{\partial z} S^{xz} \right) \right] = \\ \frac{2}{Re} \left(1 - \frac{\lambda_2}{\lambda_1} \right) \frac{\partial u}{\partial x}, \end{aligned} \quad (11)$$

respectively. Similarly, the other components of (7) and (8) can be easily obtained.

2.1 Boundary Conditions

In order to solve equations (7)-(8) it is necessary to impose boundary conditions for the velocity field on mesh boundaries. For rigid boundaries we employ the no-slip condition $\mathbf{u} = \mathbf{0}$ while at fluid entrances (inflows) the normal velocity is specified by $u_n = U_{inf}$ and the tangential velocities are set to zero, namely, $u_{m_1} = u_{m_2} = 0$, where m_1 and m_2 denote tangential directions to the inflow. At fluid exits (outflows) the Neumann condition $\frac{\partial \mathbf{u}}{\partial n} = 0$ is adopted. We consider a viscous fluid flowing in a passive atmosphere so that if we neglect surface tension forces then on the free surface the correct boundary condition is given by (see Batchelor,¹⁵ page 153)

$$n_i \cdot (\pi_{ij} \cdot n_j) = 0, \quad (12)$$

$$m1_i \cdot (\pi_{ij} \cdot n_j) = 0, \quad (13)$$

$$m2_i \cdot (\pi_{ij} \cdot n_j) = 0, \quad (14)$$

where n_i is the outward unit normal vector to the free surface and $m1_i, m2_i$ are unit tangential vectors and π_{ij} is the stress tensor $\pi_{ij} = -p\delta_{ij} + \sigma_{ij}$.

2.2 Computation of the non-Newtonian tensor S_{ik} on mesh boundaries

When solving equations (8) we shall apply a high order upwind method to approximate the convective terms. This will require the values of the non-Newtonian stress tensor on the mesh boundaries. Following the ideas presented by Tome et al.,¹ the values of S_{ik} are obtained as follows.

Computation of the non-Newtonian tensor S_{ik} on inflow boundaries: On these type of boundaries the components of the non-Newtonian tensor S_{ik} are set to zero, namely, $S_{ik} = 0, i, k = 1, 2, 3$.

Computation of the non-Newtonian tensor S_{ik} on outflow boundaries: Here we employ the homogeneous Neumann condition for S_{ik} : $\frac{\partial S_{ik}}{\partial n} = 0, i, k = 1, 2, 3$, where n represents the normal direction to the outflow.

Computation of the non-Newtonian tensor S_{ik} on solid boundaries: As rigid boundaries may be regarded as characteristics the components of the non-Newtonian tensor S_{ik} can be computed as follows.

First, by introducing the change of variables $\bar{S}_{ik} = e^{-(t/We)} \tilde{S}_{ik}$ into (8) it reduces to

$$\tilde{S}_{ik} = \frac{2}{Re} \left(1 - \frac{\lambda_2}{\lambda_1} \right) e^{(t/We)} d_{ik}. \quad (15)$$

If we consider rigid boundaries which are parallel to one of the coordinate axis then in 3 dimensions the rigid boundaries can be represented by 6 planes. These planes are easily identified as the faces of the unit cubic. For instance, considering the plane shown in figure 1 we can see that there are 2 planes corresponding to the z -axis, one has the normal vector pointing to the positive z -direction and the other is pointing to the negative z -direction. The computation of the non-Newtonian tensor S_{ik} on these planes can be easily calculated. For example, if we consider

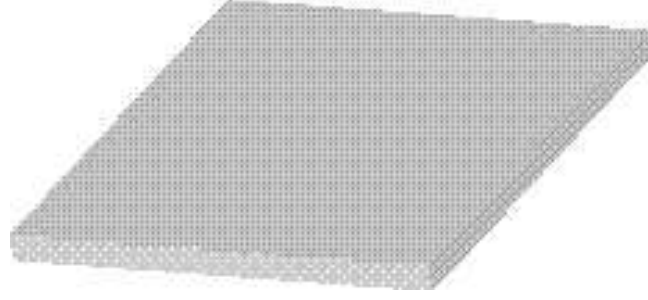


Figure 1: Rigid boundary parallel to the xy -plane.

the rigid boundary represented by the xy -plane shown in figure 1, then the no-slip condition applied to the velocity field produces $\frac{\partial}{\partial x} = \frac{\partial}{\partial y} = 0$ and using the mass conservation equation implies that $\frac{\partial w}{\partial z} = 0$. Thus, only the terms $\frac{\partial u}{\partial z}$ and $\frac{\partial v}{\partial z}$ are non-zero. In this case, equation (15) reduce to the following equations

$$\frac{\partial \tilde{S}^{xx}}{\partial t} = 2 \frac{\partial u}{\partial z} \tilde{S}^{xz}; \quad \frac{\partial \tilde{S}^{yy}}{\partial t} = 2 \frac{\partial v}{\partial z} \tilde{S}^{yz}; \quad \frac{\partial \tilde{S}^{zz}}{\partial t} = 0; \quad (16)$$

$$\frac{\partial \tilde{S}^{xy}}{\partial t} = \frac{\partial v}{\partial z} \tilde{S}^{xz} + \frac{\partial u}{\partial z} \tilde{S}^{yz}; \quad (17)$$

$$\frac{\partial \tilde{S}^{xz}}{\partial t} = \frac{\partial u}{\partial z} \tilde{S}^{zz} + \frac{1}{Re} \frac{1}{We} e^{(t/We)} \left(1 - \frac{\lambda_2}{\lambda_1}\right) \frac{\partial u}{\partial z}; \quad (18)$$

$$\frac{\partial \tilde{S}^{yz}}{\partial t} = \frac{\partial v}{\partial z} \tilde{S}^{zz} + \frac{1}{Re} \frac{1}{We} e^{(t/We)} \left(1 - \frac{\lambda_2}{\lambda_1}\right) \frac{\partial v}{\partial z}. \quad (19)$$

If we assume the initial condition $S_{ik} = 0$ then following the ideas of Tome et al.,¹ equations (16)-(19) can be solved for the components of S_{ik} and are found to be

$$S^{xx}(t + \delta t) = e^{-(\delta t/We)} S^{xx}(t) + \delta t \left[S^{xz}(t + \delta t) \frac{\partial u}{\partial z}(t + \delta t) + e^{-(\delta t/We)} S^{xz}(t) \frac{\partial u}{\partial z}(t) \right] \quad (20)$$

$$S^{xy}(t + \delta t) = e^{-(\delta t/We)} S^{xy}(t) + \frac{\delta t}{2} \left[S^{xz}(t + \delta t) \frac{\partial v}{\partial z}(t + \delta t) + S^{yz}(t + \delta t) \frac{\partial u}{\partial z}(t + \delta t) + \left(S^{xz}(t) \frac{\partial v}{\partial z}(t) + S^{yz}(t) \frac{\partial u}{\partial z}(t) \right) e^{-(\delta t/We)} \right], \quad (21)$$

$$S^{xz}(t + \delta t) = e^{-(\delta t/We)} S^{xz}(t) + \frac{1}{Re} \left(1 - \frac{\lambda_2}{\lambda_1}\right) \frac{\partial u}{\partial z}(t^*) [1 - e^{-(\delta t/We)}], \quad (22)$$

$$S^{yy}(t + \delta t) = e^{-(\delta t/We)} S^{yy}(t) + \delta t \left[S^{yz}(t + \delta t) \frac{\partial v}{\partial z}(t + \delta t) + e^{-(\delta t/We)} S^{yz}(t) \frac{\partial v}{\partial z}(t) \right] \quad (23)$$

$$S^{yz}(t + \delta t) = e^{-(\delta t/We)} S^{yz}(t) + \frac{1}{Re} \left(1 - \frac{\lambda_2}{\lambda_1}\right) \frac{\partial v}{\partial z}(t^{**}) [1 - e^{-(\delta t/We)}]. \quad (24)$$

For rigid boundaries represented by planes which are parallel to the xz - or yz -planes, the equations for calculating the components of the non-Newtonian tensor S_{ik} are obtained in a manner similar to the case of rigid boundaries parallel to the xy -plane.

3 METHOD OF SOLUTION

To solve equations (1), (7) and (8) together with the equations defining the boundary conditions we follow a procedure similar to that employed by Tome et al.¹ for two-dimensional viscoelastic flows governed by the Oldroyd-B model.

Suppose that $u_i(x_j, t_n)$, $S_{ik}(x_j, t_n)$ are known and boundary conditions for velocity and pressure are given. Then $u_i(x_j, t_{n+1})$ and $S_{ik}(x_j, t_{n+1})$, where $t_{n+1} = t_n + \delta t$, can be obtained as follows:

Step 1: Let $\tilde{p}(x_j, t_n)$ be a pressure field which satisfies the correct pressure condition on the free surface. This pressure field is computed from the normal stress condition (35).

Step 2: Compute the intermediate velocity field, $\tilde{u}_i(x_j, t_{n+1})$:

$$\frac{\partial \tilde{u}_i}{\partial t} = \frac{\partial(u_k u_i)}{\partial x_k} - \frac{\partial \tilde{p}}{\partial x_i} + \frac{1}{Re} \left(\frac{\lambda_2}{\lambda_1} \right) \frac{\partial}{\partial x_k} \left(\frac{\partial u_i}{\partial x_k} \right) + \frac{\partial S_{ik}}{\partial x_k} + \frac{1}{Fr^2} g_i. \quad (25)$$

with $\tilde{u}_i(x_j, t_n) = u_i(x_j, t_n)$ using the correct boundary conditions for $u_i(x_j, t_n)$. These equations are solved by a finite difference method which is usually, but not necessarily, explicit.

Step 3: Solve the Poisson equation

$$\frac{\partial}{\partial x_k} \left(\frac{\partial \psi}{\partial x_k} \right) = \frac{\partial \tilde{u}_k(x_j, t_{n+1})}{\partial x_k}. \quad (26)$$

The appropriate boundary conditions for this equation are²

$$\frac{\partial \psi}{\partial n} = 0 \text{ on rigid boundaries and } \psi = 0 \text{ on the free surface.}$$

Step 4: Compute the final velocity field

$$u_i(x_j, t_{n+1}) = \tilde{u}_i(x_j, t_{n+1}) - \frac{\partial \psi(x_j, t_{n+1})}{\partial x_i}. \quad (27)$$

Step 5: Compute the pressure

$$p(x_j, t_{n+1}) = \tilde{p}(x_j, t_n) + \frac{\psi(x_j, t_{n+1})}{\delta t}. \quad (28)$$

Step 6: Update the components of the non-Newtonian extra-stress tensor on inflows and outflows.

Step 7: Update the components of the non-Newtonian extra-stress tensor on rigid boundaries

Step 8: Compute the components of the non-Newtonian extra-stress tensor from:

$$S_{ik} + We \nabla S_{ik} = \frac{2}{Re} \left(1 - \frac{\lambda_2}{\lambda_1} \right) d_{ik} . \quad (29)$$

Equation (29) is solved by finite differences.

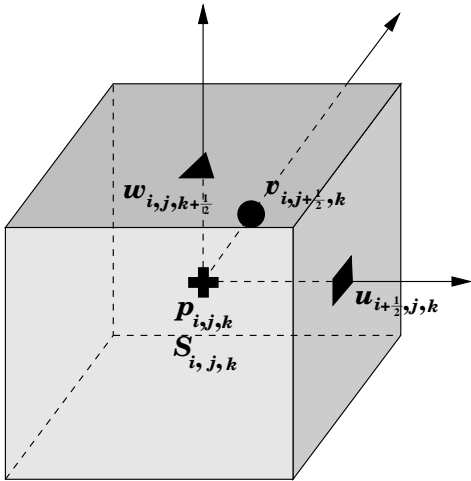
Step 9: Update the markers positions: The last step in the calculation is to move the markers to their new positions.

$$\frac{dx_i}{dt} = u_i , \quad (30)$$

for each particle. The fluid surface is defined by a piecewise linear surface composed of triangles and quadrilaterals having these marker particles on their vertices.

4 FINITE DIFFERENCE DISCRETIZATION

a)



b)

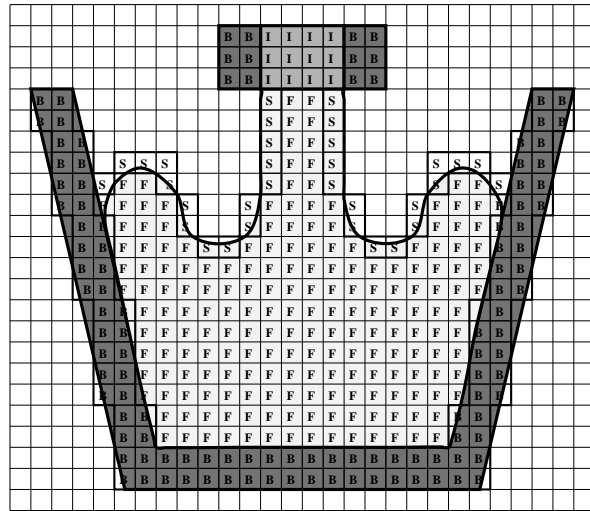


Figure 2: Staggered grid and types of cells used by Freefbw3D.

For solving **Steps 1 to 9** of the procedure presented in the previous Section we employ the following approach. A staggered grid is used. A typical cell is shown in figure 2a. The variables $p_{i,j,k}$, the potential function $\psi_{i,j,k}$ and the non-Newtonian tensor $S_{i,j,k}$ are positioned at a cell

centre while the components of the velocity field $u_{i,j,k}$, $v_{i,j,k}$ and $w_{i,j,k}$ are staggered by a translation of $\delta x/2$, $\delta y/2$ and $\delta z/2$, respectively. A scheme for identifying the free surface and the fluid region is employed. To accomodate this, the cells within the mesh are defined as empty cells (E)-cells which do not contain fluid; full cells (F)-cells which have fluid and do not have any face contiguous with empty cell faces; surface cells (S)-cells which contain fluid and have at least one face contiguous with an empty cell face; and boundary cells (B)-cell which define a rigid boundary; inflow cells (I)-cells which define an inflow boundary. An illustration of these type of cells is provided in figure 2b.

The momentum equation (25) is discretized and applied at $u-$, $v-$ and $w-$ nodes respectively. The time derivative is discretized explicitly while the Laplacian is approximated by second order differences. The pressure gradient and the divergence of $S_{\mathbf{ik}}$ are discretized by central differences. The convective terms are approximated by a high order upwind method. In this work we employ the VONOS method.¹⁶ Full details of the implementation of the VONOS method for three-dimensional flows can be found in Ferreira et al.¹⁷ For example, if we consider the x -component equation (25) (see eq. (10)), it is approximated by the following finite difference equation

$$\begin{aligned} \tilde{u}_{i+\frac{1}{2},j,k} = & u_{i+\frac{1}{2},j,k} + \delta t \left[-\mathbf{conv}(uu) - \mathbf{conv}(vu) - \mathbf{conv}(wu) - \frac{\tilde{p}_{i+1,j,k} - \tilde{p}_{i,j,k}}{\delta x} \right. \\ & + \frac{1}{Re} \left(\frac{\lambda_2}{\lambda_1} \right) \left(\frac{u_{i-\frac{1}{2},j,k} - 2u_{i+\frac{1}{2},j,k}u_{i+\frac{3}{2},j,k}}{\delta x^2} + \frac{u_{i+\frac{1}{2},j-1,k} - 2u_{i+\frac{1}{2},j,k} + u_{i+\frac{1}{2},j+1,k}}{\delta y^2} \right. \\ & + \left. \frac{u_{i+\frac{1}{2},j,k-1} - 2u_{i+\frac{1}{2},j,k} + u_{i+\frac{1}{2},j,k+1}}{\delta z^2} \right) + \frac{S_{i+1,j,k}^{xx} - S_{i,j,k}^{xx}}{\delta x} + \frac{S_{i+\frac{1}{2},j+\frac{1}{2},k}^{yx} - S_{i+\frac{1}{2},j-\frac{1}{2},k}^{yx}}{\delta y} \\ & \left. + \frac{S_{i+\frac{1}{2},j,k+\frac{1}{2}}^{zx} - S_{i+\frac{1}{2},j,k-\frac{1}{2}}^{zx}}{\delta z} + \frac{1}{Fr^2}g_x \right], \end{aligned} \quad (31)$$

where the convective terms $\mathbf{conv}(uu)$, $\mathbf{conv}(vu)$ and $\mathbf{conv}(wu)$ are approximated by the VONOS method. Terms like $S_{i+\frac{1}{2},j+\frac{1}{2},k}^{yx}$ are obtained by averaging the nearest neighbours, for instance,

$$S_{i+\frac{1}{2},j+\frac{1}{2},k}^{yx} = \frac{S_{i,j,k}^{yx} + S_{i+1,j,k}^{yx} + S_{i,j+1,k}^{yx} + S_{i+1,j+1,k}^{yx}}{4}.$$

The Poisson equation (26) is discretized at cell centres using the seven-point Laplacian, namely,

$$\begin{aligned} \frac{\psi_{i+1,j,k} - 2\psi_{i,j,k} + \psi_{i-1,j,k}}{\delta x^2} + \frac{\psi_{i,j+1,k} - 2\psi_{i,j,k} + \psi_{i,j-1,k}}{\delta y^2} + \frac{\psi_{i,j,k+1} - 2\psi_{i,j,k} + \psi_{i,j,k-1}}{\delta z^2} = \\ \frac{\tilde{u}_{i+\frac{1}{2},j,k} - \tilde{u}_{i-\frac{1}{2},j,k}}{\delta x} + \frac{\tilde{v}_{i,j+\frac{1}{2},k} - \tilde{v}_{i,j-\frac{1}{2},k}}{\delta y} + \frac{\tilde{w}_{i,j,k+\frac{1}{2}} - \tilde{w}_{i,j,k-\frac{1}{2}}}{\delta z}. \end{aligned} \quad (32)$$

Equation (32) leads to a symmetric and positive definite linear system for $\psi_{i,j,k}$. In order to solve this linear system we employ the conjugate gradient method as implemented in GENSMAC3D

(see Tome et al.⁵). The final velocities are obtained by discretizing (27) at the respective nodes, giving

$$\begin{cases} u_{i+\frac{1}{2},j,k} = \tilde{u}_{i+\frac{1}{2},j,k} - \left(\frac{\psi_{i+1,j,k} - \psi_{i,j,k}}{\delta x} \right), \\ v_{i,j+\frac{1}{2},k} = \tilde{v}_{i,j+\frac{1}{2},k} - \left(\frac{\psi_{i,j+1,k} - \psi_{i,j,k}}{\delta y} \right), \\ w_{i,j,k+\frac{1}{2}} = \tilde{w}_{i,j,k+\frac{1}{2}} - \left(\frac{\psi_{i,j,k+1} - \psi_{i,j,k}}{\delta z} \right). \end{cases} \quad (33)$$

The constitutive equation (29) is approximated by finite differences and applied at cell centres. The time derivative is discretized by the explicit Euler method. The linear spatial derivatives are approximated by central differences while the convective terms are discretized by using the high order upwind VONOS method.¹⁶ For instance, the x -component of the constitutive equation (29) as given by equation (11) is approximated by the finite difference equation

$$\begin{aligned} (S^{xx})_{i,j,k}^{n+1} &= S_{i,j,k}^{xx} + \delta t \left\{ -\mathbf{conv}(uS^{xx})_{i,j,k} - \mathbf{conv}(vS^{xx})_{i,j,k} - \mathbf{conv}(wS^{xx})_{i,j,k} \right. \\ &\quad \left. + 2 \left[\left(\frac{\partial u}{\partial x} \right)_{i,j,k} S_{i,j,k}^{xx} + \left(\frac{\partial u}{\partial y} \right)_{i,j,k} S_{i,j,k}^{xy} + \left(\frac{\partial u}{\partial z} \right)_{i,j,k} S_{i,j,k}^{xz} \right] \right\}. \end{aligned} \quad (34)$$

where

$$\left. \frac{\partial u}{\partial x} \right|_{i,j,k} = \frac{u_{i+\frac{1}{2},j,k} - u_{i-\frac{1}{2},j,k}}{\delta x}, \quad \left. \frac{\partial u}{\partial y} \right|_{i,j,k} = \frac{u_{i,j+\frac{1}{2},k} - u_{i,j-\frac{1}{2},k}}{\delta y}, \quad \left. \frac{\partial u}{\partial z} \right|_{i,j,k} = \frac{u_{i,j,k+\frac{1}{2}} - u_{i,j,k-\frac{1}{2}}}{\delta z}.$$

Expressions like $\mathbf{conv}(uS^{xx})_{i,j,k}$ represent the convective terms in (11) and are approximated by the VONOS¹⁶ scheme. The other components of S_{ik} are obtained in a similar manner.

4.1 Application of the free surface stress conditions

By using Cartesian coordinates, the boundary condition on the free surface can be written as (according to equations (12)-(14))

$$\begin{aligned} \tilde{p} &= \frac{2}{Re} \left(\frac{\lambda_2}{\lambda_1} \right) \left[\frac{\partial u}{\partial x} n_x^2 + \frac{\partial v}{\partial y} n_y^2 + \frac{\partial w}{\partial z} n_z^2 + \left(\frac{\partial v}{\partial x} + \frac{\partial u}{\partial y} \right) n_x n_y + \left(\frac{\partial w}{\partial x} + \frac{\partial u}{\partial z} \right) n_x n_z \right. \\ &\quad \left. + \left(\frac{\partial w}{\partial y} + \frac{\partial v}{\partial z} \right) n_y n_z \right] + S^{xx} n_x^2 + S^{yy} n_y^2 + S^{zz} n_z^2 + 2S^{xy} n_x n_y + 2S^{xz} n_x n_z + 2S^{yz} n_y n_z \end{aligned} \quad (35)$$

$$\begin{aligned} &\frac{1}{Re} \left(\frac{\lambda_2}{\lambda_1} \right) \left[2 \frac{\partial u}{\partial x} n_x m_{1x} + 2 \frac{\partial v}{\partial y} n_y m_{1y} + 2 \frac{\partial w}{\partial z} n_z m_{1z} + \left(\frac{\partial v}{\partial x} + \frac{\partial u}{\partial y} \right) (m_{1x} n_y + m_{1y} n_x) \right. \\ &\quad \left. + \left(\frac{\partial w}{\partial x} + \frac{\partial u}{\partial z} \right) (m_{1x} n_z + m_{1z} n_x) + \left(\frac{\partial w}{\partial y} + \frac{\partial v}{\partial z} \right) (m_{1y} n_z + m_{1z} n_y) \right] \\ &+ S^{xx} n_x m_{1x} + S^{yy} n_y m_{1y} + S^{zz} n_z m_{1z} + S^{xy} (m_{1x} n_y + m_{1y} n_x) \\ &+ S^{xz} (m_{1x} n_z + m_{1z} n_x) + S^{yz} (m_{1y} n_z + m_{1z} n_y) = 0 \end{aligned} \quad (36)$$

$$\begin{aligned}
& \frac{1}{Re} \left(\frac{\lambda_2}{\lambda_1} \right) \left[2 \frac{\partial u}{\partial x} n_x m_{2x} + 2 \frac{\partial v}{\partial y} n_y m_{2y} + 2 \frac{\partial w}{\partial z} n_z m_{2z} + \left(\frac{\partial v}{\partial x} + \frac{\partial u}{\partial y} \right) (m_{2x} n_y + m_{2y} n_x) \right. \\
& + \left. \left(\frac{\partial w}{\partial x} + \frac{\partial u}{\partial z} \right) (m_{2x} n_z + m_{2z} n_x) + \left(\frac{\partial w}{\partial y} + \frac{\partial v}{\partial z} \right) (m_{2y} n_z + m_{2z} n_y) \right] \\
& + S^{xx} n_x m_{2x} + S^{yy} n_y m_{2y} + S^{zz} n_z m_{2z} + S^{xy} (m_{2x} n_y + m_{2y} n_x) \\
& + S^{xz} (m_{2x} n_z + m_{2z} n_x) + S^{yz} (m_{2y} n_z + m_{2z} n_y) = 0
\end{aligned} \tag{37}$$

To approximate these conditions we follow the ideas employed by Tome et al.⁵ We suppose that the mesh spacing is small so that, locally, the free surface can be approximated by a planar surface. We consider three types of planar surfaces: 1D-planar surfaces, 2D-planar surfaces and 3D-planar surfaces. 1D-planar surfaces are surfaces which are perpendicular to one of the coordinate axis (x -, y - or z -axis) while 2D and 3D-planar surfaces are 45° and 60° -sloped surfaces, respectively (see figure 3). Details are given as follows:

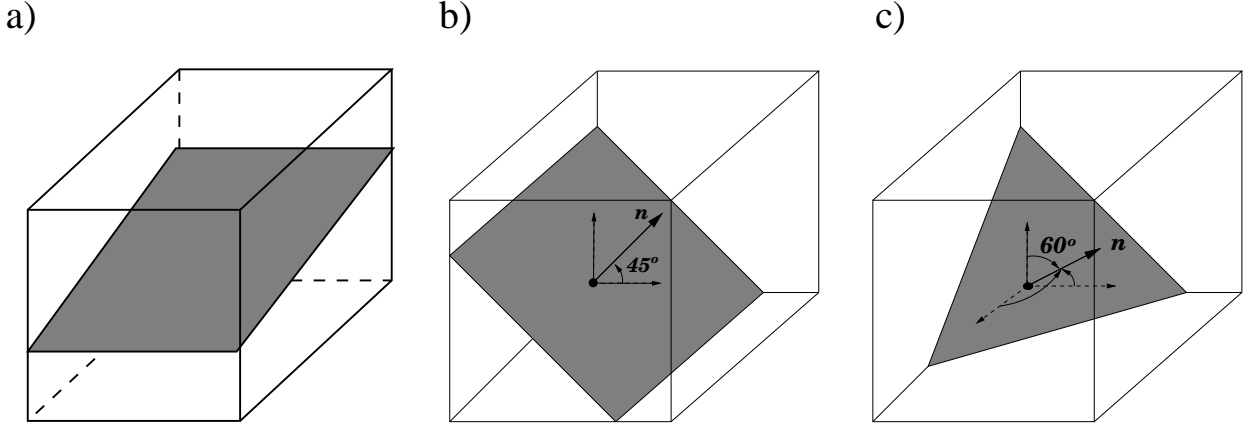


Figure 3: Types of planar surfaces: a) 1D-planar surface; b) 2D-planar surface; c) 3D-planar surface.

i) 1D-Planar surfaces: these surfaces have the normal vector pointing either to the x or y or z -direction. These surfaces are identified by surface cells having only one face in contact with an empty cell face. In these surfaces the normal vector takes the form of $(\pm 1 \ 0 \ 0)^T$ or $(0 \ \pm 1 \ 0)^T$ or $(0 \ 0 \ \pm 1)^T$. For instance, if a surface cell has the $(k + \frac{1}{2})$ -face or the $(k - \frac{1}{2})$ -face in contact with an empty cell face (see figure 2) then we assume the free surface is parallel to the xy -plane. In this case the normal vector points to the z -direction. Regarding figure 3a, the normal vector takes the form $\mathbf{n} = [0 \ 0 \ \pm 1]^T$ and we take the tangential vectors to be $\mathbf{m1} = [0 \ 1 \ 0]^T$ and $\mathbf{m2} = [1 \ 0 \ 0]^T$. In this case, the stress conditions (35)-(37) reduce to

$$\tilde{p} - \frac{2}{Re} \left(\frac{\lambda_2}{\lambda_1} \right) \frac{\partial w}{\partial z} + S^{zz} = 0 \tag{38}$$

$$\frac{1}{Re} \left(\frac{\lambda_2}{\lambda_1} \right) \left(\frac{\partial v}{\partial z} + \frac{\partial w}{\partial y} \right) + S^{yz} = 0 \tag{39}$$

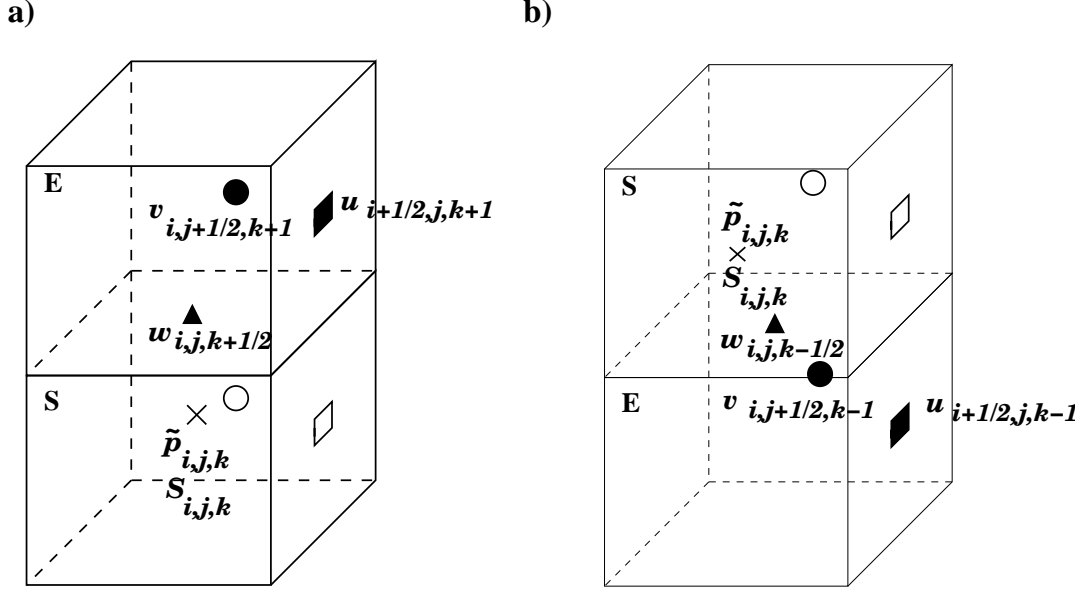


Figure 4: Surface cell having only the $(k - \frac{1}{2})$ and the $(k + \frac{1}{2})$ -face in contact with an empty cell face.

$$\frac{1}{Re} \left(\frac{\lambda_2}{\lambda_1} \right) \left(\frac{\partial u}{\partial z} + \frac{\partial w}{\partial x} \right) + S^{xz} = 0 \quad (40)$$

For instance, if we consider the surface cell shown in figure 4a the value of the pressure $p_{i,j,k}$ and the values of the velocities $w_{i,j,k+\frac{1}{2}}$, $u_{i+\frac{1}{2},j,k+1}$ and $v_{i,j+\frac{1}{2},k+1}$ are required. These are obtained as follows. By imposing mass conservation for the surface cell we obtain

$$\frac{u_{i+\frac{1}{2},j,k} - u_{i-\frac{1}{2},j,k}}{\delta x} + \frac{v_{i,j+\frac{1}{2},k} - v_{i,j-\frac{1}{2},k}}{\delta y} + \frac{w_{i,j,k+\frac{1}{2}} - w_{i,j,k-\frac{1}{2}}}{\delta z} = 0. \quad (41)$$

Now, discretizing (40) at position $(i + \frac{1}{2}, j, k + \frac{1}{2})$ we have

$$\frac{u_{i+\frac{1}{2},j,k+1} - u_{i+\frac{1}{2},j,k}}{\delta z} + \frac{w_{i+1,j,k+\frac{1}{2}} - w_{i,j,k+\frac{1}{2}}}{\delta x} = Re \left(\frac{\lambda_1}{\lambda_2} \right) S_{i+\frac{1}{2},j,k+\frac{1}{2}}^{xz} \quad (42)$$

and applying a similar discretization to (40) at position $(i, j + \frac{1}{2}, k + \frac{1}{2})$ we obtain

$$\frac{v_{i,j+\frac{1}{2},k+1} - v_{i,j+\frac{1}{2},k}}{\delta z} + \frac{w_{i,j+1,k+\frac{1}{2}} - w_{i,j,k+\frac{1}{2}}}{\delta y} = Re \left(\frac{\lambda_1}{\lambda_2} \right) S_{i,j+\frac{1}{2},k+\frac{1}{2}}^{yz}. \quad (43)$$

Equations (41)-(43) provide 3 equations for $w_{i,j,k+\frac{1}{2}}$, $u_{i+\frac{1}{2},j,k+1}$ and $v_{i,j+\frac{1}{2},k+1}$ giving

$$w_{i,j,k+\frac{1}{2}} = w_{i,j,k-\frac{1}{2}} - \frac{\delta z}{\delta x} \left(u_{i+\frac{1}{2},j,k} - u_{i-\frac{1}{2},j,k} \right) - \frac{\delta z}{\delta y} \left(v_{i,j+\frac{1}{2},k} - v_{i,j-\frac{1}{2},k} \right) \quad (44)$$

$$u_{i+\frac{1}{2},j,k+1} = u_{i+\frac{1}{2},j,k} - \frac{\delta z}{\delta x} \left(w_{i+1,j,k+\frac{1}{2}} - w_{i,j,k+\frac{1}{2}} \right) - \delta z Re \left(\frac{\lambda_1}{\lambda_2} \right) S_{i+\frac{1}{2},j,k+\frac{1}{2}}^{xz} \quad (45)$$

$$v_{i,j+\frac{1}{2},k+1} = v_{i,j+\frac{1}{2},k} - \frac{\delta z}{\delta y} \left(w_{i,j+1,k+\frac{1}{2}} - w_{i,j,k+\frac{1}{2}} \right) - \delta z Re \left(\frac{\lambda_2}{\lambda_1} \right) S_{i,j+\frac{1}{2},k+\frac{1}{2}}^{yz} \quad (46)$$

Once the velocities have been obtained, the pressure at the surface cell centre is computed from (38) yielding

$$\tilde{p}_{i,j,k} = \frac{2}{Re} \left(\frac{\lambda_2}{\lambda_1} \right) \left(\frac{w_{i,j,k+\frac{1}{2}} - w_{i,j,k-\frac{1}{2}}}{\delta z} \right) + S_{i,j,k}^{zz}. \quad (47)$$

If the surface cell has only the $(k - \frac{1}{2})$ -face in contact with an empty cell face (see figure 4b) the values of the velocities and the pressure are obtained similarly and are given by

$$w_{i,j,k-\frac{1}{2}} = w_{i,j,k+\frac{1}{2}} + \frac{\delta z}{\delta x} \left(u_{i+\frac{1}{2},j,k} - u_{i-\frac{1}{2},j,k} \right) + \frac{\delta z}{\delta y} \left(v_{i,j+\frac{1}{2},k} - v_{i,j-\frac{1}{2},k} \right) \quad (48)$$

$$u_{i+\frac{1}{2},j,k-1} = u_{i+\frac{1}{2},j,k} + \frac{\delta z}{\delta x} \left(w_{i+1,j,k-\frac{1}{2}} - w_{i,j,k-\frac{1}{2}} \right) + \delta z Re \left(\frac{\lambda_1}{\lambda_2} \right) S_{i+\frac{1}{2},j,k-\frac{1}{2}}^{xz} \quad (49)$$

$$v_{i,j+\frac{1}{2},k-1} = v_{i,j+\frac{1}{2},k} + \frac{\delta z}{\delta y} \left(w_{i,j+1,k-\frac{1}{2}} - w_{i,j,k-\frac{1}{2}} \right) + \delta z Re \left(\frac{\lambda_2}{\lambda_1} \right) S_{i,j+\frac{1}{2},k-\frac{1}{2}}^{yz}. \quad (50)$$

The application of the free surface boundary conditions for other types of 1D planar surfaces is performed similarly.

ii) 2D-Planar surfaces: These are surfaces that make a 45° with two coordinate axes. These surfaces are identified by surface cells having two adjacent faces in contact with empty cell faces. In these cells we assume that the normal vector is pointing at a direction which makes 45° with two axes, e.g. x and y or x and z or y and z and therefore we suppose that the normal vector takes the form of $\mathbf{n} = \left(\pm \frac{\sqrt{2}}{2}, \pm \frac{\sqrt{2}}{2}, 0 \right)$ or $\mathbf{n} = \left(\pm \frac{\sqrt{2}}{2}, 0, \pm \frac{\sqrt{2}}{2} \right)$ or $\mathbf{n} = \left(0, \pm \frac{\sqrt{2}}{2}, \pm \frac{\sqrt{2}}{2} \right)$. To illustrate the application of the free stress conditions for this type of surfaces we take the case of a surface cell having the $(i + \frac{1}{2})$ and $(k + \frac{1}{2})$ -faces in contact with empty cell faces (see figure 5). For these cells we assume that the unit normal takes the form $\mathbf{n} = \left(\frac{\sqrt{2}}{2}, 0, \frac{\sqrt{2}}{2} \right)$ and the tangential vectors are taken to be:

$$\mathbf{m1} = \left(\frac{\sqrt{2}}{2}, 0, -\frac{\sqrt{2}}{2} \right) \quad \text{and} \quad \mathbf{m2} = (0, 1, 0).$$

Introducing these vectors into equations (35)–(36) we obtain

$$\tilde{p} = \frac{1}{Re} \left(\frac{\lambda_2}{\lambda_1} \right) \left[\frac{\partial u}{\partial x} + \frac{\partial w}{\partial z} + \frac{\partial u}{\partial z} + \frac{\partial w}{\partial x} \right] + \frac{1}{2} S^{xx} + \frac{1}{2} S^{yy} + S^{xy}, \quad (51)$$

$$\frac{1}{Re} \left(\frac{\lambda_2}{\lambda_1} \right) \left[\frac{\partial u}{\partial x} - \frac{\partial w}{\partial z} \right] + S^{xy} + S^{yz} = 0 \quad (52)$$

respectively. As we can see in figure 5, the values of $u_{i+\frac{1}{2},j,k}$, $w_{i,j,k+\frac{1}{2}}$ at the empty-cell faces and the pressure $\tilde{p}_{i,j,k}$ are required. These are obtained by applying (52) and the mass conservation equation at the surface cell centre in which case we obtain

$$\frac{1}{Re} \left(\frac{\lambda_2}{\lambda_1} \right) \left[\frac{u_{i+\frac{1}{2},j,k} - u_{i-\frac{1}{2},j,k}}{\delta x} - \frac{w_{i,j,k+\frac{1}{2}} - w_{i,j,k-\frac{1}{2}}}{\delta z} \right] + S^{xy} + S^{yz} = 0 \quad (53)$$

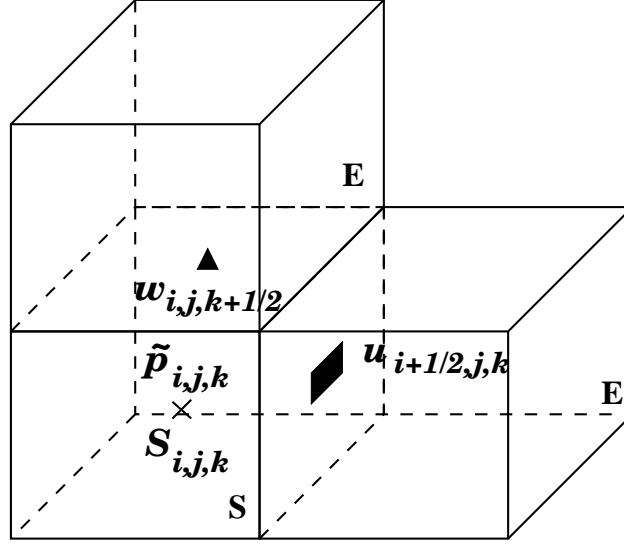


Figure 5: Surface cell with $(i + \frac{1}{2})$ and $(k + \frac{1}{2})$ -faces contiguous with E-cells.

$$\frac{u_{i+\frac{1}{2},j,k} - u_{i-\frac{1}{2},j,k}}{\delta x} + \frac{w_{i,j,k+\frac{1}{2}} - w_{i,j,k-\frac{1}{2}}}{\delta z} = - \left(\frac{v_{i,j+\frac{1}{2},k} - v_{i,j-\frac{1}{2},k}}{\delta y} \right) \quad (54)$$

respectively. Solving (53) and (54) for $u_{i+\frac{1}{2},j,k}$ and $w_{i,j,k+\frac{1}{2}}$ we obtain

$$u_{i+\frac{1}{2},j,k} = u_{i-\frac{1}{2},j,k} - \frac{1}{2} \frac{\delta x}{\delta y} \left(v_{i,j+\frac{1}{2},k} - v_{i,j-\frac{1}{2},k} \right) + \frac{\delta x}{4} \frac{\lambda_1}{\lambda_2} \frac{1}{Re} \left(S_{i,j,k}^{zz} - S_{i,j,k}^{zz} \right) \quad (55)$$

and

$$w_{i,j,k+\frac{1}{2}} = w_{i,j,k-\frac{1}{2}} - \frac{1}{2} \frac{\delta z}{\delta y} \left(v_{i,j+\frac{1}{2},k} - v_{i,j-\frac{1}{2},k} \right) + \frac{\delta z}{4} \frac{\lambda_1}{\lambda_2} \frac{1}{Re} \left(S_{i,j,k}^{xx} - S_{i,j,k}^{zz} \right) . \quad (56)$$

Once the velocities at the empty-cell faces have been computed the pressure at the surface cell centre is calculated by (51), namely

$$\begin{aligned} \tilde{p}_{i,j,k} = & \frac{1}{Re} \left(\frac{\lambda_2}{\lambda_1} \right) \left[\frac{u_{i+\frac{1}{2},j,k} - u_{i-\frac{1}{2},j,k}}{\delta x} + \frac{w_{i,j,k+\frac{1}{2}} - w_{i,j,k-\frac{1}{2}}}{\delta z} \right. \\ & + \frac{1}{2} \left(\frac{u_{i+\frac{1}{2},j,k} + u_{i-\frac{1}{2},j,k} - u_{i+\frac{1}{2},j,k-1} - u_{i-\frac{1}{2},j,k-1}}{\delta z} \right. \\ & \left. \left. + \frac{w_{i,j,k+\frac{1}{2}} + w_{i,j,k-\frac{1}{2}} - w_{i-1,j,k+\frac{1}{2}} - w_{i-1,j,k-\frac{1}{2}}}{\delta x} \right) \right] + \frac{1}{2} S_{i,j,k}^{xx} + \frac{1}{2} S_{i,j,k}^{yy} + S_{i,j,k}^{xy} . \quad (57) \end{aligned}$$

Other configurations of surface cells having only two adjacent faces in contact with empty cell faces are treated similarly.

iii) 3D-Planar surfaces: 60°-sloped planar surface: These surfaces are defined to have the local unit vector making 60° with the coordinate axes. They are identified by surface cells

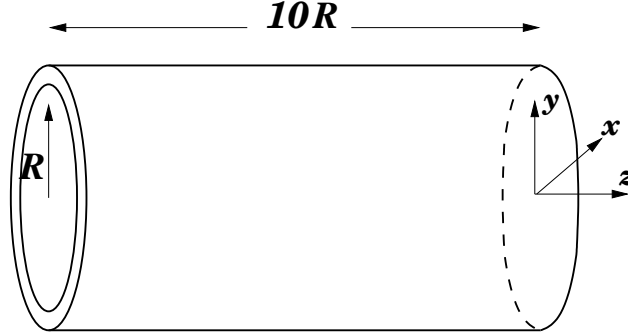


Figure 7: Numerical simulation of the flow of an Oldroyd-B fluid in a pipe: 3D case.

lated the pressure is computed by discretizing (58) at the surface cell centre. Details of the finite difference equations involved can be found in Tomé et al.⁵

5 VALIDATION RESULTS

The finite difference equations discussed in Section 4 were implemented into the Freeflow3D code (see Castelo et al.¹⁸) in order to simulate unsteady free surface flow of an Oldroyd-B fluid.

To validate the numerical method presented in this paper we simulated the flow of an Oldroyd-B fluid in a pipe. We considered a pipe of radius R and having a length of $10R$ (see figure 7) and impose a steady state parabolic flow at the pipe entrance given by

$$W(x, y) = 2 \left[R^2 - \sqrt{x^2 + y^2} \right], \quad u = v = 0. \quad (62)$$

In this case, it can be shown that the components of the extra stress tensor S_{ik} are given by

$$S^{xy} = 0, \quad S^{xz} = \frac{1}{Re} \left(1 - \frac{\lambda_2}{\lambda_1} \right) \frac{\partial w}{\partial x}, \quad S^{yz} = \frac{1}{Re} \left(1 - \frac{\lambda_2}{\lambda_1} \right) \frac{\partial w}{\partial y}, \quad (63)$$

$$S^{xx} = S^{yy} = 0, \quad S^{zz} = 2 \frac{We}{Re} \left(1 - \frac{\lambda_2}{\lambda_1} \right) \left[\left(\frac{\partial w}{\partial x} \right)^2 + \left(\frac{\partial w}{\partial y} \right)^2 \right]. \quad (64)$$

To simulate this problem, the following input data were employed: $R = 1\text{m}$, $\delta x = \delta y = \delta z = 0.1\text{m}$ (mesh size of $20 \times 20 \times 200$). Gravity was neglected. The scaling parameters were $R = 1\text{m}$, $U = 1\text{ms}^{-1}$, $\nu = 1\text{m}^2\text{s}^{-1}$, $\lambda_1 = 1$, $\lambda_2 = 0.5$, giving $Re = 1$ and $We = 1$.

We ran the Freeflow-3D code with the data above. We started with an empty pipe and injected fluid at the pipe entrance until the pipe was full and the steady state was reached. Figure 8 displays the fluid flow configuration at selected times while figure 9 shows the variation of the velocity w , the components of the non-Newtonian tensor S^{xz} and S^{zz} and the first normal stress difference $N1$ at the plane xz passing in the centre of the pipe. Figure 9 also shows these values at the cross-section of the pipe situated at the position $z = 2.5$. We can observe in figure 9 that the isolines are all parallel indicating that the steady state was reached.

Figure 10 displays the numerical and the analytical values of $w(x, y)$, S^{zz} , S^{xz} and S^{yz} along the line parallel to the x -axis passing at the center of the cross-section of the pipe situated at $z = 2.5$. We can see that the agreement between the two solutions is very good.

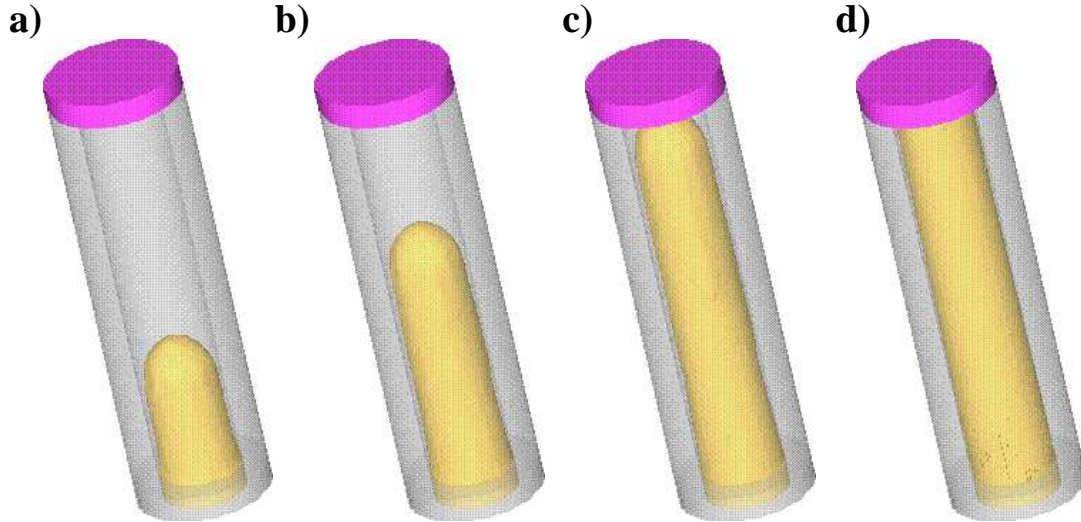


Figure 8: Fluid flow configuration computed at different times: a) $t = 2.5$, b) $t = 5.0$, c) $t = 9.0$ and d) $t = 20$.

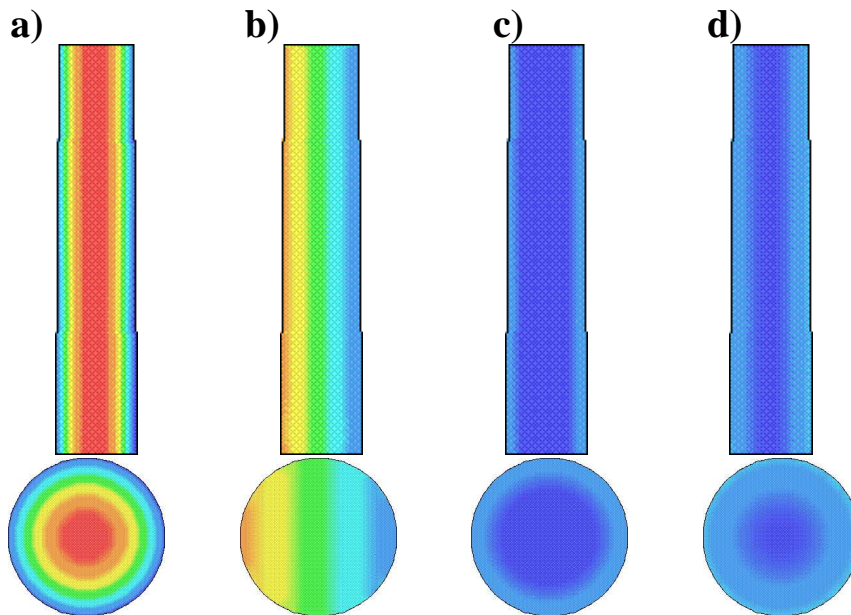


Figure 9: Contour lines at $t = 20$. a) Velocity field, b) S^{xz} ; c) S^{zz} ; d) $N1$.

6 NUMERICAL SIMULATION OF VISCOELASTIC FREE SURFACE FLOWS

To demonstrate that the technique presented in this paper can cope with viscoelastic free surface flows we applied it to simulate the extrudate swell of an Oldroyd-B fluid. We considered the

time-dependent flow of an axisymmetric jet flowing inside a tube and then extruded in air. The no-slip condition is imposed on the tube walls while fully developed flow is assumed at the tube entrance (see (62)-(64)). On the fluid free surface the full stress conditions (see Section 4.1) are applied. The components of the non-Newtonian stress S_{ik} on the wall of the tube are computed by the equations derived in Section 2.2. The flow domain is the same as that shown in figure 7. To simulate this problem the following input data were employed: tube radius $R = 1\text{cm}$, tube

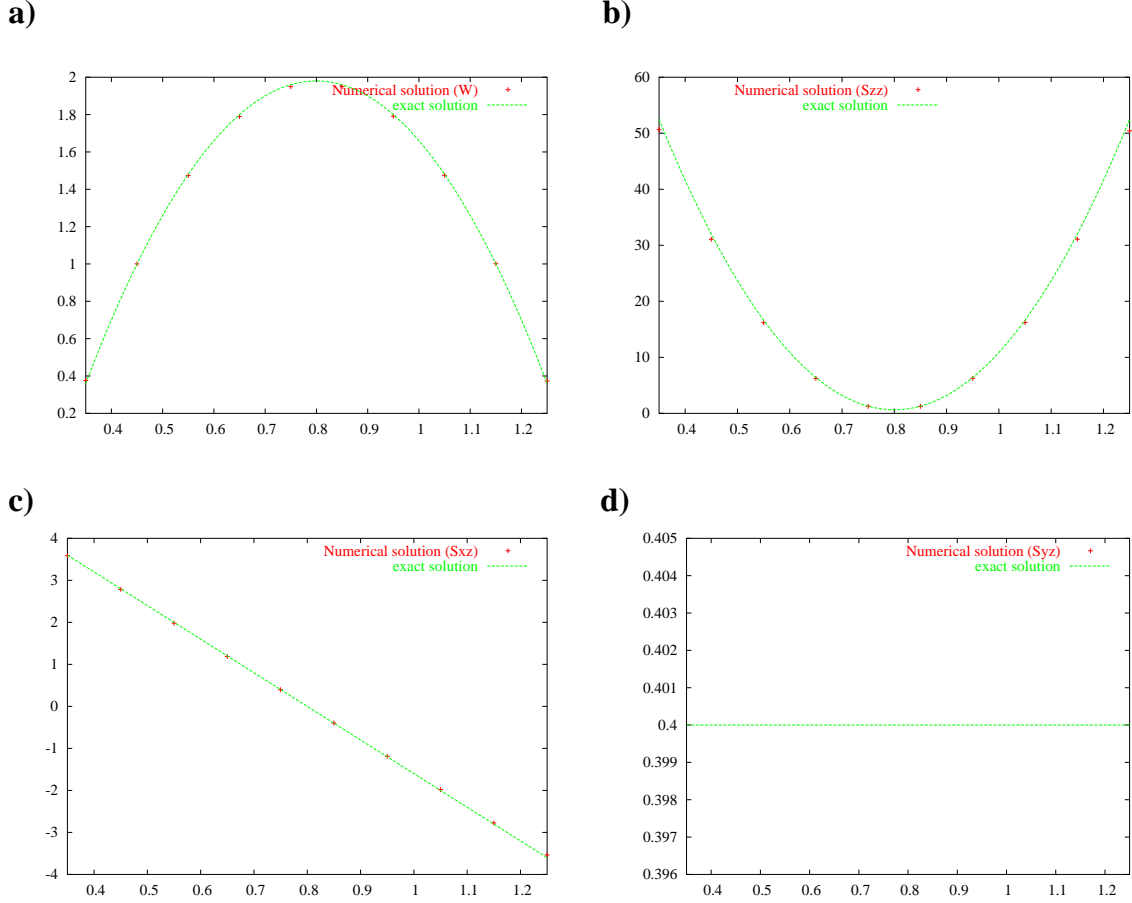


Figure 10: Comparison between the analytic and the numerical solutions at the cross section of the pipe $z = 2.5$ along the line parallel to the x -axis. **a)** Velocity field, **b)** S^{zz} ; **c)** S^{xz} ; **d)** S^{yz} .

length $L = 3R$, $\delta x = \delta y = \delta z = 0.1\text{cm}$ (20×100 cells), Poisson tolerance $\text{EPS} = 10^{-10}$. Fluid definition: $\nu_0 = 0.010 \text{ m}^2\text{s}^{-1}$, $\lambda_1 = 0.01\text{s}$. The scaling parameters were R , $U = 1$, ν_0 and λ_1 , giving $Re = UR/\nu_0 = 1$ and $We = \lambda_1 U/R = 1$. To demonstrate that the code can deal with the Oldroyd-B model, we used these input data and performed three simulations. In the first simulation the value of $\lambda_2 = 0.9\lambda_1$ was used and in the second simulation we used $\lambda_2 = 0.75\lambda_1$ while in the third simulation we chose $\lambda_2 = 0.5\lambda_1$. We point out that the effective Weissenberg number for the Oldroyd-B model is given by (see Yoo and Na³): $We_{\text{effect}} = \left(1 - \frac{\lambda_2}{\lambda_1}\right) We$. Thus, in these simulations we used $We_{\text{effect}} = 0.1, 0.25, 0.5$, respectively. The results of these

simulations are shown in figure 11. Figure 11 shows the jet flowing inside the tube and then being extruded into the air.

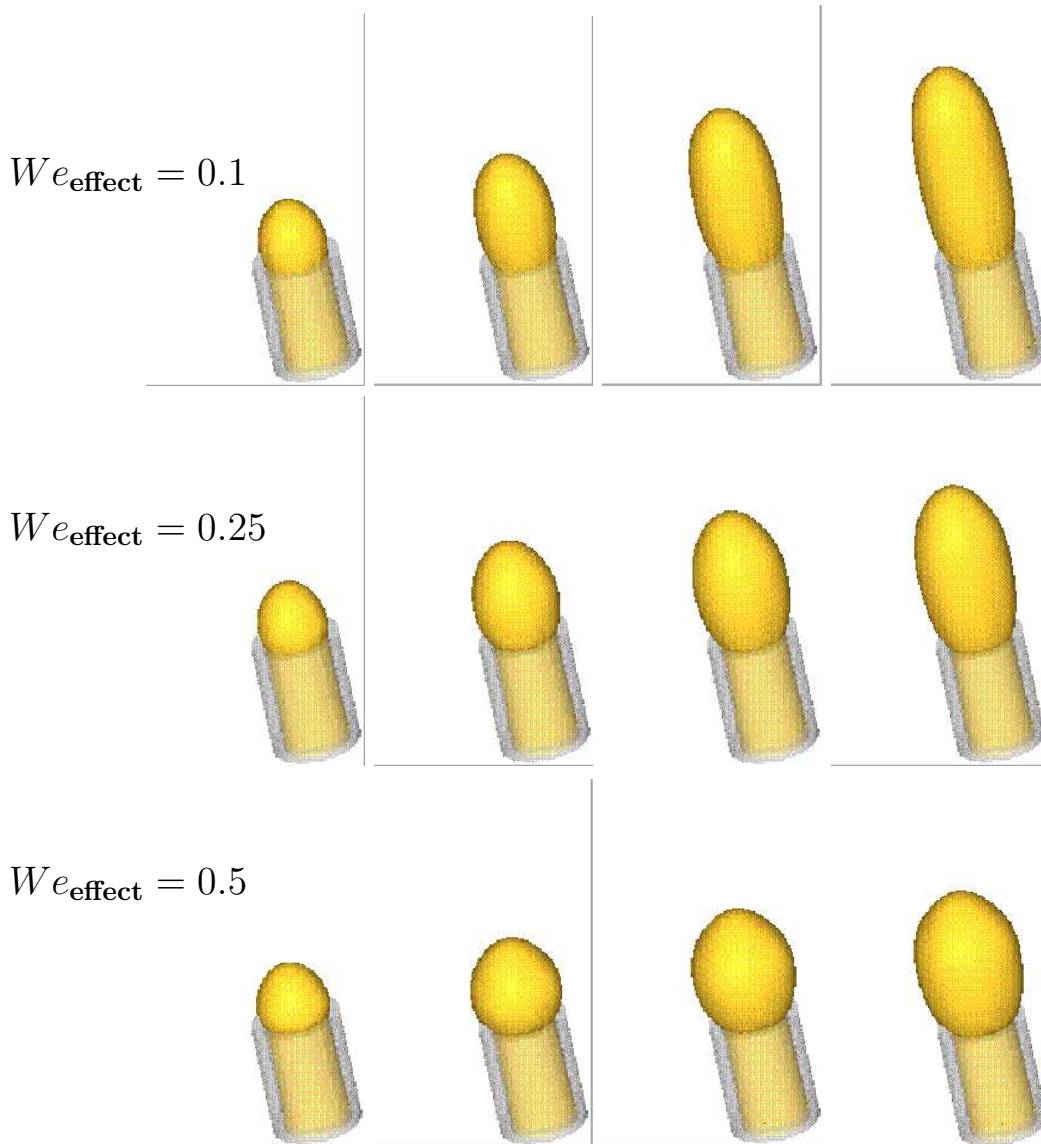


Figure 11: Fluid flow visualization of the simulation of the extrudate swell for increasing We_{effect} . Times shown are (from left to right) $t = 0.04\text{s}$, 0.06s , 0.08s and 0.12s , respectively.

For the time $t = 0.04\text{s}$ (first column) the jet is just leaving the tube and the differences between the three simulations are not noticeable. However, at later times the jet is extruded into the air and the differences between the three simulations become more noticeable. This is particularly true for the case of $t = 0.12\text{s}$ (last column) where we can observe that the results for the case of $We_{\text{effect}} = 0.5$ present a much larger swelling than the results of the other two simulations. Indeed, at the time $t = 0.12\text{s}$, the maximum swelling ratio ($S_r = R_{\text{max}}/R$) for

the three simulations were 28% for $We_{\text{effect}} = 0.1$, 46% for $We_{\text{effect}} = 0.25$ and 59% for $We_{\text{effect}} = 0.5$. These results show that the technique presented in the paper can deal with high elastic fluids governed by the Oldroyd-B constitutive equation.

CONCLUDING REMARKS

This paper presented a numerical method for solving three-dimensional free surface flows governed by the Oldroyd-B model. The numerical technique developed herein is based on the finite difference method and employed the Marker-and-Cell approach to represent the fluid free surface. The finite difference equations developed in this work have been implemented into the FreeFlow3D code of Castelo et al.¹⁸ extending FreeFlow3D to viscoelastic free surface flows. The numerical method was validated by simulating the flow inside a pipe and compared with the corresponding analytic solution. The agreement between the two solutions was very good. In addition, the numerical simulation of the extrudate swell for various values of the effective Weissenberg number was given.

ACKNOWLEDGMENTS

We gratefully acknowledge the support given by Fapesp (grant 2000/03385-0) and CNPq (grants 523141/94 and 474040/2003-8).

REFERENCES

- [1] M.F. Tomé, N. Mangiavacchi, J.A. Cuminato, A. Castelo, and S. McKee. A numerical technique for solving unsteady viscoelastic free surface flows. *J. Non-Newtonian Fluid Mech.*, **106**, 61–106 (2002).
- [2] Tomé M. F. and McKee S. Gensmac: A computational marker-and-cell method for free surface flows in general domains. *Journal of Computational Physics*, **110**, 171–186 (1994).
- [3] J.Y. Yoo and Y. Na. A numerical study of the planar contraction flow of a viscoelastic fluid using the simpler algorithm. *J. Non-Newtonian Fluid Mech.*, **30**, 89–106 (1991).
- [4] Castelo A., Mangiavacchi N., Tomé M.F., Cuminato J.A., Fortuna A.O, Oliveira J., and S. McKee. Surface tension implementation for gensmac2d. *Journal of the Brazilian Society of Mechanical Sciences*, **23**, 523–534 (2001).
- [5] Tomé M. F., A. Castelo, Cuminato J. A., Mangiavacchi N., and McKee S. Gensmac3d: A numerical method for solving unsteady three-dimensional free surface flows. *International Journal for Numerical Methods in Fluids*, **37**(7), 747–796 (2001).
- [6] G. Mompean and M. Deville. Unsteady finite volume of oldroyd-b fluid through a three-dimensional planar contraction. *J. Non-Newtonian Fluid Mech.*, **72**, 253–279 (1997).
- [7] S.C. Xue, N. Phan-Thien, and R.I. Tanner. Three-dimensional numerical simulation of viscoelastic flows through planar contractions. *J. Non-Newtonian Fluid Mech.*, **74**, 195–245 (1998).
- [8] P. J. Oliveira and F. T. Pinho. Analytical solution of fully developed channel and pipe flow

- of phan-thien-tanner fluids. *J. Fluid Mech.*, **387**, 271–280 (1999).
- [9] T.N. Phillips and A.J. Williams. Viscoelastic flow through a planar contraction using a semi-lagrangian finite volume method. *J. Non-Newtonian Fluid Mech.*, **87**, 215–246 (1999).
- [10] E. Brasseur, M.M. Fyrillas, G.C. Georgiou, and M.J. Crochet. The time-dependent extrudate-swell problem of an oldroyd-b fluid with slip along the wall. *J. Rheol.*, **42**(3), 549–566 (1998).
- [11] E. Mitsoulis. Three-dimensional non-newtonian computations of extrudate swell with the finite element method. *Comput. Methods Appl. Mech. Engrg.*, **180**, 333–344 (1999).
- [12] V. Ngamaramvaranggul and M.F. Webster. Viscoelastic simulations of stick-slip and die-swell flows. *Int. J. Numer. Meth. Fluids*, **36**, 539–595 (2001).
- [13] K. B. Sunwoo, S. J. Park, S. J. Lee, K. H. Ahn, and S. J. Lee. Numerical simulation of three-dimensional viscoelastic flow using the open boundary condition method in coextrusion process. *J. Non-Newtonian Fluid Mech.*, **99**, 125–144 (2001).
- [14] D. Rajagopalan, R. Armstrong, and R. Brown. Finite element methods for calculation of steady viscoelastic flow using constitutive equations with newtonian viscosity. *J. Non-Newtonian Fluid Mech.*, **36**, 159–192 (1990).
- [15] G. K. Batchelor. *An Introduction to Fluid Dynamics*. Cambridge University Press, (1967).
- [16] A. Varonos and G. Bergeles. Development and assessment of a variable-order non-oscillatory scheme for convection term discretization. *Int. J. Numer. Meth. Fluids*, **26**, 1–16 (1998).
- [17] V.G. Ferreira, M.F. Tome, N. Mangiavacchi, A. Castelo Filho, J.A. Cuminato, A.O. Fortuna, and S. McKee. High order upwinding and the hydraulic jump. *Int. J. Numer. Meth. Fluids*, **39**, 549–583 (2002).
- [18] Castelo A., Tomé M.F., Cuminato J.A., and S. McKee. Freeflow: An integrated simulation system for three-dimensional free surface flows. *Computing and Visualization in Science*, **2**, 199–210 (2000).